Non Equilibrium Phase Transitions in Intermetallics

G. MARTIN and P. BELLON - Cerem, Section de Recherches de Métallurgie Physique - CE-S, 91191, Gif sur Yvette cedex, France

Abstract

When intermetallics are operating under conditions where the atomic order is permanently disturbed from it's thermodynamical optimum, phase equilibria may no more be predicted from the classical free energy functions. Nevertheless, under simplifying assumptions, one may construct a new function, playing a similar role for assessing the respective stability of various phases: the latter is based on microscopic data such as atomic jump frequencies and interatomic binding energies, but does not imply an internal energy! After giving some examples of practical relevance of the present theory, we present the guiding ideas on which it relies, show it's present limitations and some examples where it is applied, at least as a qualitative guide, for rationalizing e.g. complex processing techniques such as mechanical alloying or subtile irradiation effects on the stability of intermetallics.

Riassunto

Quando i composti intermetallici operano in condizioni in cui l'ordine atomico risulta turbato in modo permanente rispetto all'ottimo termodinamico, gli equilibri di base non sono più predicibili dalle classiche funzioni di entalpia libera.
Nondimeno, partendo da ipotesi semplificate si può costruire una nuova funzione avente un analogo ruolo per valutare la stabilità delle singole fasi: questa funzione poggia su dati microscopici, come la frequenza di salti atomici e le energie di legame interatomico, senza tuttavia implicare un'energia interna! Dopo aver dato esempi di rilevanza pratica della presente teoria, si espongono i concetti informatori su cui essa poggia, se ne indicano le attuali limitazioni e si forniscono alcuni esempi di pratica applicazione, almeno a titolo orientativo, per razionalizzare, ad es., complesse tecniche di trattamento, come l'alligamento meccanico o gli effetti di irradiazioni sottili sulla stabilità dei composti intermetallici.

Introduction

Materials Science and Technology offer many examples where intermetallics or compound semiconductors are driven or maintained in non equilibrium configurations: intermetallics in alloys under irradiation, e.g. Fe Zr_2 in Zircalloy used as a cladding material in pressurized water nuclear reactors, or any of the compounds produced by ion implantation or ion beam mixing in advanced technologies are typical examples. In such compounds, atoms are permanently ejected from their equilibrium position by nuclear collisions, while thermal jumps tend to restore some degree of atomic order. Other examples, including the fatigue of super-alloys and the production of new phases by mechanical alloying, will be discussed in the next section. For the sake of simplicty, we call such compounds "driven systems" or "driven intermetallics": indeed, such systems are driven away from the usual thermodynamic equilibrium by a permanent dynamical forcing (nuclear collisions, plastic shear etc.).

Under such circumstances, a rather involved question arises: assuming the driven alloy may achieve several steady-state configurations, is there a means to predict the respective stability of the latter, much in the same way as thermodynamics, in principle, allows to predict the more stable configuration of an alloy. The relevance of this question is not purely academic, since, answering it would reveal the control parameters of the state of the alloy under dynamical conditions, and help, e.g. predicting the alloy stability from simulation experiments, or optimizing processing conditions.

During the last couple of years, definite progresses have been achieved in the theory of the stability of such "driven intermetallics". The second section gives the principle of this theory which relies on a very simple idea. In an "un-driven system", which obeys thermodynamics, Gibbs hypothesis (equiprobability of all micro-states of equal energy) permits to express the probability of a macro-state at fixed temperature as the exponential of a free energy function. The most probable macro state corresponds to that with the minimum free energy. This implies that, under thermodynamic equilibrium, the system explores its configuration space with a trajectory such that it spends more time in the more probable macro state; the latter trajectory is dictated by the thermally activated jumps of the atoms on the lattice. Under external forcing, the trajectory of the system, in the same configuration space, is modified by the occurrence of atomic jumps which are not only activated thermally, but also by the external forcing. The very same technique which is used to interpret the free energy function in terms of the thermally activated jump-frequencies, can be used to construct an "effective free energy" function giving the respective probability of two macro-states when both types of jumps (thermally activated and forced) are operating simultaneously.

The "effective free energy" thus constructed helps deciding which is the more stable steady-state under given forcing conditions. Dynamical equilibrium phase diagrams may thus be constructed. Such diagrams are described in section three: they often exhibit unexpected features.

Finally, we stress the hopes and limitations of this new theory, the inductive nature of which is worth mentioning.

Examples of "driven compounds"

Among the many examples where a crystalline compound is maintained in a dynamical equilibrium by some sort of external forcing, we briefly discuss here four typical cases: compounds under irradiation, coherent two-phase alloys under cyclic fatigue, intermetallics under ball-milling (as occurs in the preparation of compounds by mechanical alloying) and compound semi-conductors when grown by metal organic vapor phase epitaxy. The common features to all these examples will become clearer below. We begin by compounds under irradiation because the atomistic processes, there, are particularly simple and well understood: such systems therefore represent a prototype to which others may be compared.

Compounds under irradiation

When an heavy particle enters a solid, it is slowed down by two types of processes: electronic excitations and nuclear collisions [1].

In insulating materials, electronic excitations may produce atomistic disorder by several mechanisms, such as coulombic explosion (temporarily unscreened ions violently repel one-another) or non-radiative recombination of excitons (a very effective defect production mechanism e.g. in CaF_2 under 100 KeV electron irradiation). In metallic solids, because of the very effective screening of electronic perturbations, similar processes only occur for extreme values of electronic slowing down (typically 10 to 100 MeV/μm) which can nowadays be achieved in the very high energy heavy ion accelerators like GANIL in France or GSI in Germany [2].

Nuclear collisions, on the contrary, are very effective in creating atomistic disorder in metals: provided the energy transferred to an atom is larger than some displacement threshold (typically 25 eV), the atom will be expelled from its lattice site and leave a vacancy behind, while a self interstitial atom will be created some lattice sites away. If the expelled atom has itself a high enough kinetic energy, it may transfer part of this energy to a second atom, which will be also displaced: a "displacement cascade" thus occurs. During this process, several atoms exchange lattice site: the number thereof depends on the cascade density, and may be rather large (more than one hundred atoms per vacancy created in dense cascades). Nuclear collisions then result in two competing processes: the forced exchange of lattice site for many atoms and the creation of some point defects which, because of their thermally activated mobility, help restoring the local chemical order which has been destroyed by the forced jumps.

As an example, Fig. 1, taken from the work of Van Tandeloo and Amelinckx, exhibits the time evolution (from the left to the right) of the crystallographic structure of the Ni_4Mo compound under 1 MeV electron irradiation, at three different irradiation temperatures. The top sequence corresponds to a low temperature irradiation: the ordered compound is transformed into a disordered FCC solid solution, as evidenced by the disappearance of the superlattice reflections spots in the electron diffraction pattern. The intermediate sequence corresponds to an irradiation at intermediate temperature: the initially disordered solid solution gets ordered, with a symmetry which can be described by a concentration wave of wave vector 1/4(420). At higher temperature (bottom sequence), the same irra-

diation induces a transformation from the above structure into one with a longer wavelength: 1/5(420); the latter is indeed the thermal equilibrium crystallographic structure. At still higher temperature (not shown in the picture), the final structure is the disordered solid solution, as in the absence of irradiation, above the order-disorder transition temperature. Clearly, the crystallographic structure in dynamical equilibrium under irradiation depends on the irradiation temperature; complementary experiments show it also depends on the irradiation flux and on the cascade size [3]. This type of experiment, slightly idealized, serves as a guide for building the theory of the stability of driven compounds to be presented in section two.

Coherent two phases alloys under cyclic loading

A well known class of high strength two phases alloys is provided by the socalled super-alloys. The most popular ones are Nickel base (e.g. PE16 or CMSX2 ...); more recently Aluminium Lithium super-alloys have also been processed. The strength of such alloys is mainly due to a high volume fraction of a coherent second phase made of an intermetallic such as Ni_3Al, or respectively Al_3Li. Such intermetallics exhibit a high yield stress in particular at high temperature. Fig. 2 taken from the work of Y. Brechet [4] on fatigue resistance of Al Li superalloys, shows that under appropriate conditions of cyclic loading, the plastic strain concentrates in "persistent slip bands" (PSB), and that, under the influence of the permanent back and forth movement of dislocations in these bands, precipitates dissolve; the solute so released re-precipitates in the matrix along the PSB. It is claimed that on cutting the compound, dislocations induce disorder which decreases the cohesive energy of the precipitate. It is known that point defects are created by dislocation movements: although the atomistic mechanisms are less precisely known than for nuclear collisions, it is seen that the stability criterion of the two phases alloys in the PSB may be addressed in terms similar to those discussed above for alloys under irradiation, i.e. the competition between forced disordering and thermally activated reordering. The problem here is more complex because of the spatial non uniformity of the external forcing (PSB).

Formation of metastable phases by high energy ball milling

For many years it has been known that high energy ball-milling could be used for producing ultrafine dispersions of oxides in various types of alloys. Such reinforced composite materials are commonly manufactured. During the last decade, however, it was realized that the same technique is suitable for inducing chemical mixing of several elements at the atomistic scale, starting from elemental powders, or from a multiphase master-alloy. One thus gets crystalline compounds with extended solid solubility, or amorphous alloys in composition ranges where rapid quenching is ineffective (e.g. at stoichiometry for congruently melting compounds!) [5]. Ball-milling, by shearing, fracturing, re-welding the elemental powders, promotes mixing at the atomistic level, much in the same way as the "baker transformation" mixes the trajectories in chaotic dynamical systems. It was argued that the mixture of elemental crystalline powders would decrease it's free energy, by enhanced solid state diffusion, down to some level higher than the equilibrium state, for unexplained reasons. However, it was recently shown that the same amorphous solid solution may be obtained either by mechanically alloying elemental powders, or by milling the equilibrium intermetallic compound with the same composition (Fig. 3). In the former case, the free energy of the final state is lower than that of the initial state, while the reverse is true in the latter case. Clearly, the metal under ball-milling achieves some dynamical equilibrium state; it is still an open question to know whether the stability of such states may be described with the simple scheme discussed in sub-sections (a) and (b), above.

Compound semi-conductors grown by vapor phase epitaxy

The free surface of a compound semi-conductor when exposed to a metal organic vapor, receives atoms of several species; the latter diffuse on the surface and stabilize in a fully disordered or partially or fully ordered structure which, because of the growth of the crystal, gets buried into the bulk of the material. Seen in the moving frame of reference attached to the free surface, this overall process can

again be seen as a competition between forced disordering (at a rate proportional to the growth rate of the crystal) and thermally activated ordering. Indeed, Bellon and col. [6] identified a case of growth *induced* ordering in GaInP on GaAs substrates: GaIn ordering on the Ga sublattice was observed under (growth) temperature conditions where the ordered bulk phase is thermodynamically unstable; surface ordering had been quenched into the bulk.

As a summary, in the above context, one is interested in predicting not only the steady state degree of ordering of the compound when exposed to external forcing, but mainly, when several steady states are possible, which of these is more stable. The former question can be answered by simple rate equations describing the competition between the driven decrease of the order parameter and the thermally activated increase thereof. Such models also give information on the *local* stability of the steady state: when prepared in a state close to the steady state, does the compound evolve towards or away from that state? But such models are unable to predict the *global* stability, i.e. the respective stability of two *locally* stable steady states. This latter question is more involved and requires a stochastic treatment of the problem. Such a treatment has been developed during the last two years and is summarized in the next section.

Theory of the stability of "driven compounds"

Basic principle

The theory we developed, rests on the following idea (Fig. 4): under thermal equilibrium conditions, i.e. in the absence of external forcing, atomic migration occurs in the compound (e.g. by vacancy diffusion mechanism) in such a way that the various microscopic configurations of the alloy are explored with a probability equal to what is predicted by standard thermodynamics, i.e., their Boltzman's weight:

$$P_i = \exp\ (-\beta E_i)/Z \tag{1}$$

where subscript (i) labels a microscopic configuration with energy E_i, β is the inverse of the temperature, in energy units, Z is the normalization constant called the configurational sum. In other words, there is a means to deduce eq. 1 from a miscroscopic description of atomic jumps in an alloy at thermal equilibrium. As will be seen, from the kinetics, we only get a slightly less detailed information, namely:

$$P_i/P_j = \exp\ \{-\beta(E_i - E_j)\} \tag{2}$$

Assuming the above step to be achieved, it will be a simple matter to replace in the kinetic model, the thermally activated jump frequencies by the sum of the former and the frequency of the forced jumps. An expression similar to eq. 2 will result, but with a complicated function replacing E; the latter can nevertheless be computed from atomistic data, much in the same way as E can be estimated in the classical models (e.g. Bragg Williams approximation) for solid solutions. In practice, one is interested by a coarser description of the state of the alloy, e.g. as defined by a Bragg Williams order parameter S; summing eq. 1 on all the values of i which correspond to the same value of S yields the probability for observing a given value of S:

$$P(S) = \exp\ \{-\beta\ F(S)\}/Z \tag{3}$$

where F(S) is a free energy function which is proportional to the size of the system and writes:

$$F(S) = E(S) - kT\ \mathrm{Ln}\ \{w(S)\} \tag{4}$$

where w(S) is the number of configurations with a given S, k Boltzmans's constant and T the temperature. It can be shown that F(S) is proportional to the number of sites in the sample (extensive quantity). The *respective stability* of two states characterized by S_1 and S_2 is estimated from their respective probability: $P(S_1)/P(S_2)$, i.e. from the difference in their free energy functions. Under external forcing, the latter difference is replaced by that of a new function (an "effective free energy") which can be computed from atomistic parameters to the same degree of sophistication as "mean field" models for the free energy.

In the following we show in slightly more details how to proceed in cases of increasing complexity.

Simple case: one single order parameter

Consider first the order disorder transition in the Body. Centered Cubic lattice, as is the case in β brass: the BCC lattice is made of two simple cubic lattices shifted by one half the cube diagonal. At stoichiometry, an A B compound (e.g. CuZn or NiTi etc...) will be fully ordered, provided the temperature is low enough compared to the critical temperature for the order-disorder transition: A atoms are all located on one of the simple cubic lattices (we call it sublattice #1), B atoms on the second (sublattice #2). At intermediate temperatures, or away from the stoichiometric composition, some A atoms will be located on sublattice #2 and vice versa. We consider that the state of the alloy is sufficiently well described by the knowledge of one number, S, the difference in occupancy ratio of the two sublattices e.g. by A atoms. If the fraction of sites on sublattice #k which are occupied by A atoms is X_k (k = 1 or 2), then $S = X_1 - X_2$; the overall alloy composition is $C = (X_1 + X_2)/2$. At stoichiometry ($C = 1/2$), the fully ordered state gives $S = 1$, the fully disordered one yields $S = 0$.

Consider a large number of samples with the same composition and the same number of lattice sites, Ω. The proportion $P(N_1)$ of those systems where N_1 A atoms are located on sublattice #1 changes in time because in some samples one A atom on sublattice 1 exchanges with one B atom on sublattice 2 while in others, one A atom on sublattice 2 will exchange with one B atom on sublattice 1: $P(N_1)$ is increased by the former process and decreased by the latter. The time evolution of $P(N_1,t)$, where t is the time, is governed by a master equation:

$$\begin{aligned} \partial P(N,t)/\partial t = \; & \{P(N-1)W_{N-1/N} - P(N)W_{N/N-1}\} \\ & - \{P(N)W_{N/N+1} - P(N+1)W_{N+1/N}\} \end{aligned} \tag{5}$$

For simplicity we have omitted the subscript (1) and the time t in the argument of P in eq. 5; $W_{N/N-1}$ represents the fraction of samples with N A atoms on sublattice #1 in which, within a time unit, one A atom on sublattice #1 exchanges with one atom B on sublattice #2 (N changes into N-1). Obviously, $W_{N/N-1}$ is proportional to the exchange frequency of AB pairs in an alloy in the macro state N.

We are interested in the stationary solution of eq. 5 (steady state), i.e. in finding the function P(N) which makes the right hand side of eq. 5 identical to zero. The latter can be viewed as the difference of two probability fluxes, or two fluxes of samples, along the N axis: the first line corresponds to the flux from N − 1 to N, the second one from N to N + 1.

In the absence of forcing, i.e. in a purely thermodynamic case, general arguments (time reversibility of the microdynamic of the system) permits to state that each of the two fluxes is zero in equilibrium (i.e. in steady state); we thus have the so called "detailed balance condition":

$$P(N)/P(N+1) = W_{N-1/N}/W_{N/N-1} \tag{6}$$

and, by iterating eq. 6,

$$P(N)/P(N_0) = \prod_{n=N_0+1}^{N} W_{n-1/n}/W_{n/n-1} \tag{7}$$

Without going into details, each transition probability, W_{ij}, is the product of two terms:

— the number of paths linking the initial to the final state i.e. the number of bonds between A and B atoms on the appropriate sublattices; the latter is proportional to the number of lattice sites in the sample;
— times the exchange frequency of such an AB pair, $\Gamma_{AB}(N)$.

The latter is a thermally activated quantity. If we choose as an activation energy the energy required to extract the AB pair from it's initial configuration and to bring it into some saddle point configuration, it is easy to prove that eq. 7 reduces to eqs. 3-4, where the internal energy, E(S), is computed as a sum of the same bound energies as the activation energy, and the configurational entropy, $kLn\{w(S)\}$, is estimated to the same level of sophistication as the number of appropriate AB bonds in the kinetic model. The link between a kinetic interpretation and classical thermodynamics is thus established.

When the system is driven, the exchange frequency of AB pairs, is now the sum of the thermally activated frequency, $\Gamma_{AN}(N)$, and of the forced frequency, Γ_{dr}, independent of temperature. The master equation (5) still holds with this new expression of the exchange frequency in the transition probabilities W. But there is no general argument anymore to write eq. 6: detailed balance is no more automatically warranted. However in the simple case studied here, a sample with all A atoms on the same sublattice cannot move towards a larger value of N: as a consequence, under steady state conditions, each flux in eq. 5 is zero as in the un-driven case. Therefore, eq. 7 still holds but with the appropriate expression for the W's. In other words, the respective stability of two macro states of the driven system is given by:

$$P(S)/P(S_0) = \exp\ \{\Omega[\varphi(S) - \varphi(S_0)]\} \tag{8}$$

with:

$$\Omega[\varphi(S) - \varphi(S_0)] = \sum_{n=N_0+1}^{N} \mathrm{Ln}\ \{W_{n-1/n}/W_{n/n-1}\} \tag{9}$$

The terms in the right hand side of eq. 9 do not rearrange as simply as in the undriven case, but the summation can be performed numerically for a given atomistic model of the forced jump frequency: the function $\varphi(S)$ depends now not only on temperature but also on the *intensity of the external driving*, expressed by a dimensionless parameter, G, the ratio of the frequency of forced to thermally activated jumps: $G = \Gamma_{dr}/\langle\Gamma_{AB}\rangle$. Fig. 5 gives an example of computed values of $\varphi(S) - \varphi(S_0)$ for an hypothetical stoichiometric AB compound with a critical ordering temperature at 1000K and prepared at 260K under an external forcing of 4.6 (i.e. the frequency of forced jumps is 4.6 the average frequency of thermally activated jumps). As can be seen, two locally stable steady states are predicted (maxima of φ): a fully disordered one ($S = 0$), a partially ordered one ($S = 0.85$). The partially ordered state is more stable than the disordered one, as revealed by the higher value of the maximum.

At higher temperature or higher forcing, the reverse is true: the disordered state is more stable than the ordered one. Figure 6 shows how does the order-disorder temperature decay with increasing the external forcing.

An interesting feature, with practical consequences, is worth mentioning. It is known that in the un-driven case, the transition between the BCC and the B2 structure (CuZn type) is of second order, i.e. proceeds homogeneously, without a nucleation barrier: the disordered state is either stable (above the critical temperature Tc) or unstable (below Tc). Such is not always the case under forcing: in the case exemplifield in fig. 5, both disordered and ordered states are locally stable; the transition is of first order! As seen on fig. 6 the shift from first — to second — order transition occurs at a well defined *tricritical point*, the theory of which is given in ref. 7. Similar computations, when done at all compositions, yield the phase diagram depicted on fig. 7.

Beyond the tricritical point, the transition is first order: it should proceed by the nucleation and growth of domains. Phase separation (i.e. the coexistence of two phases with distinct compositions and states of order) is expected! This would correspond to phase separation induced by external forcing.

Indeed, a simple kinetic model, based on the same AB exchange frequencies as used in the above stochastic theory, helps delineating the two-phases field in the temperature-concentration diagram at given forcing intensity. Fig. 8 is an example computed at $G = 4.55$ (the forced jumps are 4.55 more frequent than the thermally activated ones). A more general theory of this two-phases field is currently under development.

As a summary, the very simple case addressed here, shows that the relative stability of phases can be assessed under external forcing, and that unexpected features are revealed by this new treatment. The technique can also address more complicated situations which we discuss in the next two sections.

Multidimensional order parameter

In the previous example, the macro state of the system was defined by two variables, X_1 and X_2, the occupation ratio of sublattices 1 and 2 by A atoms. But for a fixed overall composition, assuming the alloy to be homogeneous reduced the number of degrees of freedom to one, the Bragg Williams order parameter S. As was noticed, this very peculiarity helped to take advantage of eqs. 6, and 7, and to derive the stochastic potential $\varphi(S) - \varphi(S_0)$, eqs. 8-9.

In most cases, however, the state of the alloy is described by more than one order parameter: think of the Face Centered Cubic structure, e.g. in super-alloys: the FCC lattice is formed of four simple cubic lattices shifted by one half the face diagonal. Four order parameters at least are required for specifying the macro-state of the alloy: the occupation ratio, e.g. by A atoms, of each of the four sublattices, X_1, X_2, X_3, X_4. Keeping the concentration fixed still leaves three independent order parameters. The well known $L1_2$ structure (Cu_3Au) is defined by one order parameter, since three sublattices (the centers of the cube faces) have the same occupation ratio. Similarly for the $L1_0$ structure (CuAu) in which the occupation ratios of the sublattices are equal two by two. But nothing warrants that, under external forcing, the steady state of the alloy will be a pure $L1_0$ or a pure $L1_2$ structure: it could be that the four sublattices equilibrate one-another at some intermediate structure. Also in the BCC case discussed above, when we observe phase separation, the concentration in one phase is no more fixed: the two degrees of freedom must be relaxed.

Under such circumstances, the master equation (eq. 5) still holds, but N must be understood as a vector, **N**, with (for the FCC lattice) coordinates N_1, N_2, N_3, N_4, the number of A atoms on each four sublattices. Also, the right hand side of eq. 5 becomes more complicated since the variation of $P(\mathbf{N})$ results from the unbalances in fluxes in four directions. The argument holds whatever the number of sublattices. Under steady state conditions, in the *un-driven* case, the detailed balance argument (eq. 6) still holds, and applying the same procedure as above, the link between the kinetic model and equilibrium thermodynamics can again be established. However, in the *driven* case, nothing warrants anymore that detailed balance holds, and indeed it can be proven that it does not for certain kinetic models. We are thus left with the problem of finding a steady-state solution of eq. 5, with a known expression for the transition probabilities W.

Without going into much details, let us briefly summarize a technique which turned out to be useful to achieve this goal [8]. The right hand side of the master equation is seen to consist of differences of quantities evaluated at neighboring values of N_i. If instead of the integer N_i, we use the occupation ratio, $X_i = N_i/\Omega$, a continuous variable, the right hand side of eq. 5 can be Taylor expanded to infinite order in $1/\Omega$ ("Kramers Moyal expansion"). As noticed by Kubo [9], since we look for a solution of the type:

$$P(\mathbf{X}) = P_0 \exp\{\Omega\varphi(\mathbf{X})\} \tag{10}$$

all terms must be kept in the expansion. It is found that the function $\varphi(\mathbf{X})$ is solution of:

$$0 = \sum_{\varepsilon_k} [-W(\mathbf{X} \rightarrow \mathbf{X} + \boldsymbol{\varepsilon}_k)\{1 - \exp(\boldsymbol{\varepsilon}_k . \nabla \varphi)\}] \tag{11}$$

where the $\boldsymbol{\varepsilon}_k$ are the vectors pointing to all the macro-states which can be reached from state $\mathbf{X}$. Eq. 11 is strongly non linear, and difficult to solve, for the time being, although there are some good hopes to succeed in the near future. Up to now, it has been very useful in the following case.

In the FCC lattice, it is found from a simple kinetic model, that the steady states of the driven system are pure $L1_2$ $(X_1 \neq X_2 = X_3 = X_4)$ or pure $L1_0$ $(X_1 = X_2 \neq X_3 = X_4)$ or the fully disordered $(X_1 = X_2 = X_3 = X_4 = 0)$ structures. It is easily seen that the disordered state is the center of symmetry of the order parameter space, while representative points of the $L1_2$ structure are located on three-fold symmetry axes and of $L1_0$ on two-fold axes. The latter axes intersect at the center of symmetry. For comparing the relative stability of such steady states, it therefore suffices to know the values of $\varphi(\mathbf{X})$ along the latter symmetry axes. For symmetry reasons, along such axes, all components of $\nabla\varphi$ transverse to the axis are zero. We are left with a simple integration of $\partial\varphi/\partial S$, where S is the coordinate along the symmetry axis.

When applied to the FCC lattice, the above technique allowed to compute the equilibrium phase diagram of several phases such as $L1_2$, $L1_0$ [8], or D1a and $LiFeO_2$ type [10], the stability of which has been studied under irradiation, in the particular case of Ni_4Mo [3].

"Cascade size" effects

In the preceding sections, the forced atomic jumps were assumed to occur one at a time: in the master equation, all transitions changing N_i by more than one unit could thus be omitted. In practice, however, forced jumps occur by bursts: under irradiation, up to several hundreds of atoms exchange position at once in a dense displacement cascade; such is certainly also the case under ball milling conditions. Are the prediction of the theory affected by such effects, which we call "cascade size effects", by analogy with irradiation? Cascade size effects cannot be taken into account in simple deterministic chemical rate models (which only handle mean jump frequencies), but can be straightforwardly included in the present stochastic theory.

Indeed, if more than one (say b), forced jumps occur at once, the occupation N_i of sublattice # i can change by any integer k ranging from $-b$ to $+b$. A master equation similar to eq. 5 still be written, but the right hand side will include a summation over k. The solution of eq. 5 is slightly more involved than when $b = 1$, but can be obtained with the same technique as in the previous section, at least for not too large values of b. For large b's, a technique less rigorous than Kubo's ansatz could be used, at least for one dimensional order parameters: it consists in truncating the Kramers Moyal expansion to second order (Fokker Planck equation). Although this technique is not self consistent, it gives a reasonable answer, for one dimensional problems only [7,11].

Qualitatively, increasing b increases the noise in the system, i.e. has similar effects as increasing temperature. In fact the effect is more subtile: increasing b keeping all other parameters constant (i.e. temperature, composition and the intensity of the driving, G), keeps the steady states unchanged, but affects the respective stability, of those steady states which are *locally stable*. In other words, the local maxima of $\varphi(S)$ occur at the same values of S, but their relative height may be reversed on varying b. For first order transition lines, the larger b, the more extended the stability domain of the disordered phase: for the B2 transition on the BCC lattice (fig. 7) increasing b shifts the first order transition line down towards the spinodal ordering line. Other examples will be given in the next section.

Dynamical-equilibrium phase diagrams

Computed diagrams

Apart from the B2 transition on the BCC lattice discussed above, several transitions have been studied on the FCC lattice. Unexpected features are found, and are depicted on fig. 9.

As an example, in the stoichiometric A_3B compound the equilibrium $L1_2$ (Cu_3Au) structure is predicted to be destabilized to the benefit of the $L1_0$ (CuAu) structure in a specific region of the phase diagram, shown in fig. 9a. Notice that the reduced forcing on the ordinate axis is denoted G_0 instead of G as before: G_0 is the temperature independent part of G. Indeed, the thermally activated atomic jump frequency in G, is the product of the point defect mobility times the defect concentration. For systems under irradiation, the latter can be estimated from simple defect balance equations. The existence and extension of the domain of stability for the $L1_0$ structure depends on the details of the jump model.

Another interesting example is provided by the Ni_4Mo stoichiometric compound, the experimental behavior of which was depicted in the first section. Depending on the temperature and driving intensity, G_0 which scales as the square root of the irradiation flux, three distinct structures may be stabilized: the disordered solid solution, the short range ordered structure (SRO), the long range ordered structure (LRO). For computing the stability fields of these structures, the model was adjusted to the experimental results of Banerjee et al. [2b]. As can be seen, when the cascade size increases (from $b = 1$ to 100), the stability domain of the long range ordered phase shrinks to the benefit of that of the short range ordered structure. Experimental check of this prediction is underway.

Experimental diagrams

To our knowledge, full phase diagrams as depicted on figs. 8-9, have not yet been experimentally established for intermetallics.

About ten years ago, dynamical equilibrium phase diagrams had been established for *phase separation* in solid solutions (Al base and Ni base solid solutions under irradiation) [12]. They indeed exhibit an irradiation flux dependence of the solubility limit. The atomistic mechanisms altering phase stability in this case, were however quite distinct from those discussed in the present article: irradiation sustains a supersaturation, hence fluxes of point defects towards elimination or recombination centers. The latter induce solute fluxes in the same (or the opposite) direction and hence solute accumulation at (or away from) the above centers. Solute accumulation, when it exceeds the solubility limit, triggers precipitation. A model of these processes has been established, but it could not be phrased in terms of a stochastic potential as used in the present theory.

For the time being, we are left with rationalizing qualitative features, from what is predicted by our theory. As an example, it is well known that amorphization by irradiation is "easier" (i.e. occurs on a broader temperature range, on a larger variety of compounds) in the presence of large displacement cascades (heavy ion vs light ion or electron irradiations). Similar trends exist for disordering induced dissolution of precipitates under irradiation. This is reminiscent of the cascade size effect predicted by our theory. Unexpected coexistence of amorphous and crystalline phases under irradiation has also been reported: fig. 8 is an example of irradiation induced coexistence between an ordered and a disordered phase; the amorphous phase can be viewed as an ultimately disordered structure.

The above way of thinking is currently being applied to ball milling induced amorphization. Using an instrumented vibrating frame grinder, the milling conditions required for amorphizing an $Ni_{10}Zr_7$ compound have been determined at room temperature. As seen on fig. 10 taken from the work by Chen et al., amorphization only occurs beyond a minimum power injected into the system. It is reasonable to assume that the driving parameter G increases with the injected power, although a more detailed knowledge of the atomistic processes involved in the forced mixing, would help making this relation more quantitative. Temperature effects are currently being studied.

More generally, one may suspect that the external forcing, in many processing or operating conditions of materials, is proportional to the injected power density. Fig. 11 gives typical values estimated for materials under irradiation or during plastic deformation, or during ball milling. It is worth noticing that for the broad range of values covered, alterations of phase stability have been reported under irradiation, and are to be expected under other types of forcing.

Conclusion

A slight idealization of atomistic exchanges in a compound under external forcing, permits to construct a theoretical framework for estimating the relative stability of various compound structures under dynamical conditions. The classical free energy function, which can be estimated from atomic pair interactions, is replaced by a new function, which involves the same pair interactions, but with a different combination thereof, and the intensity of the external forcing in the form of a forced atomic jump frequency.

Based on this theory, known features of phase stability under irradiation are rationalized, e.g. the strong effect of cascade size on compound stability; unexpected effects are also predicted, such as the stabilization of unexpected crystallographic structures, or a phase separation driven by the disordering of a compound.

The above framework gives hopes for clarifying the effect of processing conditions on the end product in complex alloy preparation techniques or predicting long term stability of compounds in complex operating conditions.

Acknowledgements

The stimulating atmosphere developed by our colleagues at Section de Recherches de Métallurgie Physique in Saclay is gratefully acknowledged.

References

[1] Lehmann, Chr. *Interaction of Radiation with Solids*, North-Holland, Amsterdam, 1977.

[2] Audouard, A. and 14 co-authors. The contribution of electronic losses to radiation damage in metallic materials. *Radiation Effects and Defects in Solids*, 110 (1989), 113-115.

[3a] Van Tandeloo, G. and S. Amelinckx. Ordering in alloys under electron irradiation. In H.I. Aaronson, D.E. Laughlin, R.F. Sekerka and C.M. Wayman (Eds), *Solid-Solid Phase Transformations*, AIME, New York, 1982, pp. 305-309.

[3b] Banerjee, S., K. Urban and M. Wilkens. The transition from the short-range to the long-range ordered state in Ni_4Mo under electron irradiation. Same ref. as above, pp. 311-315.

[4] Brechet, Y., F. Louchet, C. Marchionni and J.L. Verger-Gaugry. Experimental (TEM and SEM) investigation and theoretical approach to the fatigue-induced dissolution of ∂' precipitates in a 2.5wt% Al-Li alloy. *Phil. Mag.*, 56 (1987), 353-366.

[5a] Chen, Y., R., Le Hazif and G. Martin. Ball milling amorphization in a vibrating frame grinder. *J. de Phys. Colloques*, 51 (1990), C4 273-279.

[5b] Martin, G. and E. Gaffet. Mechanical alloying: for from equilibrium transition? Same ref. as above, C4 71-77.

[6] Bellon, P., J.P. Chevalier, E. Augarde, J.P. Andre and G. Martin. Substrate driven ordering microstructure in $Ga_xIn_{1-x}P$ alloys. *J. Appl. Phys.* 66 (1988), 2388-2394.

[7] Bellon, P. and G. Martin. Cascade effects in a non equilibrium transition with metallurgical relevance. *Phys. Rev.* B39 (1989), 2403-2410.
[8] Haider, F., P. Bellon and G. Martin. Non equilibrium transition in driven A_3B compounds with FCC lattice: a multivariate master equation approach. *Phys. Rev.* in the press.
[9] Kubo, R., K. Matsuo and K. Kitahara. Fluctuation and relaxation of macrovariables. *J. Stat. Phys.*, 9 (1973), 51-96.
[10] Bellon, P. and G. Martin. Cascade effect on respective stability of ordered phases in Ni_4Mo under irradiation. *J. Less Com.Metals*, 146 (1988), 465-475.
[11] Bellon, P., F. Haider and G. Martin. Cascade size effects on phase stability under irradiation: a stochastic description. In *Radiation Materials Science*. Proc. of an international conference held in Alushta, USSR, (1990), in the press.
[12] Martin, G., R. Cauvin and A. Barbu. Effects of radiation damage on phase stability and transformations. In same as reference 3, pp. 257-279.

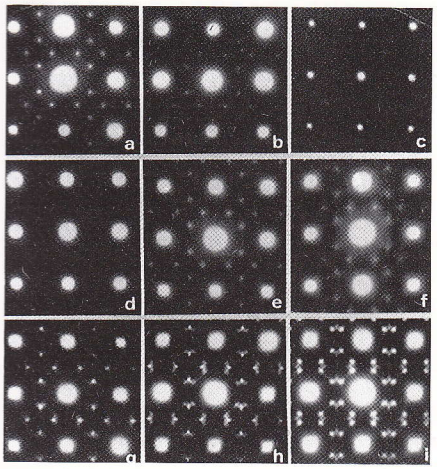

Fig. 1:
Evolution of the chemical order in the intermetallic compound Ni_4Mo under 1 MeV electron irradiation at various temperatures: time increases from the left to the right; the top, intermediate and bottom sequences respectively correspond to low, intermediate and high irradiation temperatures. The figures represents electron diffraction patterns; notice the stabilization of three different compound structures, depending on irradiation temperature: the disordered FCC solid solution at low temperature, the 1/4 [420] concentration wave at intermediate temperature, the 1/5 [420] wave at higher temperature (from Van Tandeloo et al. [2]).

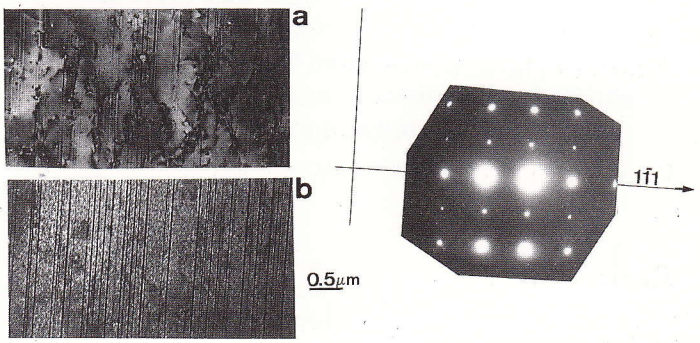

Fig. 2:
Persistent slip bands in an Al Li super alloy under cyclic loading. The white contrast corresponds to Al_3Li coherent precipitates, with $L1_2$ structure: notice that the precipitates are dissolved in the persistent slip bands, and that the Lithium so released has reprecipated at the border between ther PSB's and the matrix (courtesy of Y. Brechet).

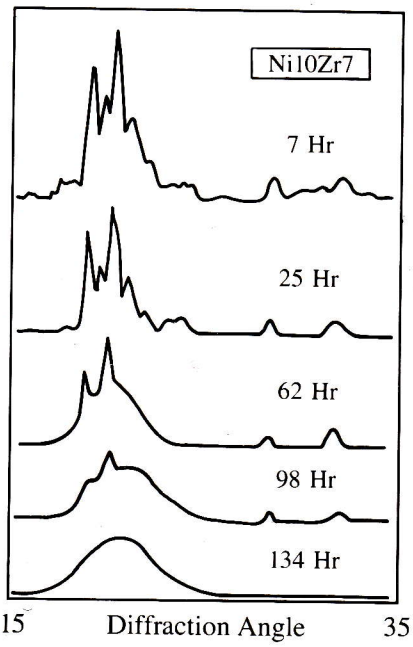

Fig. 3:
Transformation of a crystalline intermetallic compound ($Ni_{10}Zr_7$) into an amorphous solid solution by high energy ball milling, in a vibrating frame grinder. The X ray diffraction patterns reveal the crystalline structure which gets progressively distorted. At larger time (here 124 hours in the bottom spectrum), an amorphous structure is obtained (from CHEN YING'S work [5]: the latter is stable on thermal annealing at temperatures below the crystallization temperature.

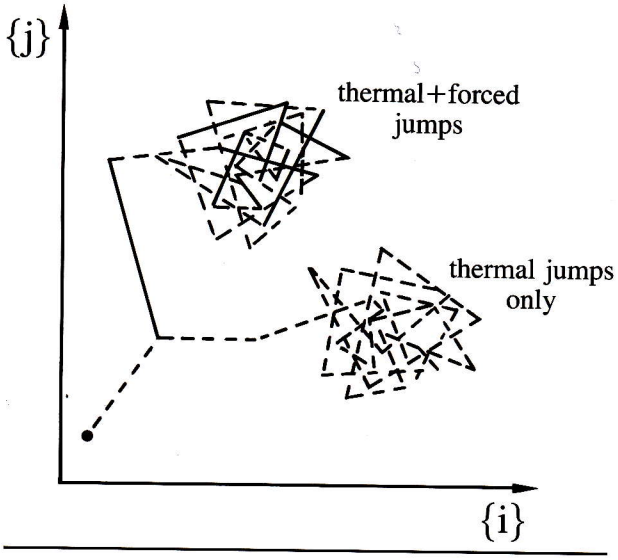

Fig. 4:
Exploration of the configuration space (schematical) under thermal conditions [dotted line) and driven conditions (full line); the various regions of the configuration space are not explored with the same frequency under both sets of conditions.

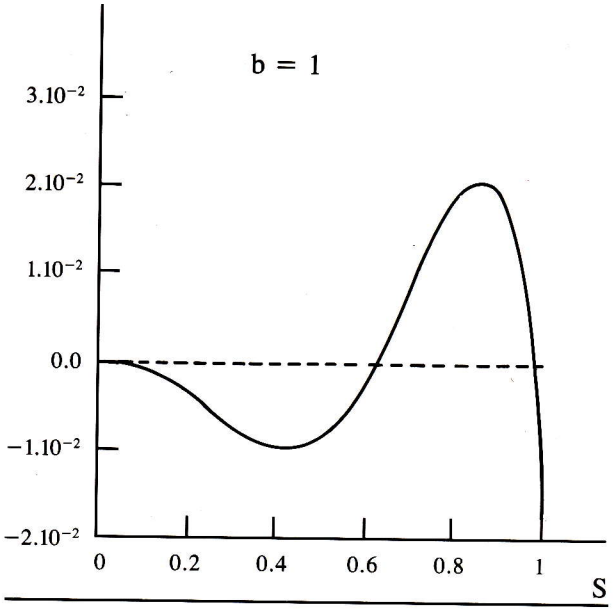

Fig. 5:
Computed values of $\varphi(S) - \varphi(0)$ for a compound with a BCC lattice and critical temperature for the order disorder transition of 1000K (in the absence of forcing). The computation is performed at a reduced temperature of .26 (i.e. 260K) and a forcing intensity of 4.6 (i.e. the forced atomic jumps are 4.6 times more frequent than the thermally activated ones). The higher maximum at S = .85 corresponds to the more stable phase (B2 or CsCl structure). The lower maximum at S = 0 corresponds to a metastable solid solution on the BCC lattice.

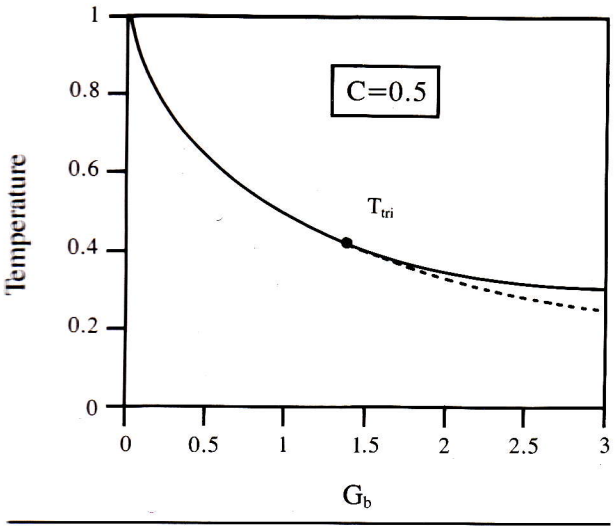

Fig. 6:
Drop of the B2 order-disorder transition temperature for increasing values of the forcing. The temperature is scaled to the critical temperature at zero forcing; the forcing intensity, G, is the frequency of forced atomic jumps relative ot that of thermally activated ones. Beyond the *tricritical point*, the transition is first order, i.e. below the transition line, the disordered state is locally stable. The latter become unstable below the *ordering spinodal* (dotted) line.

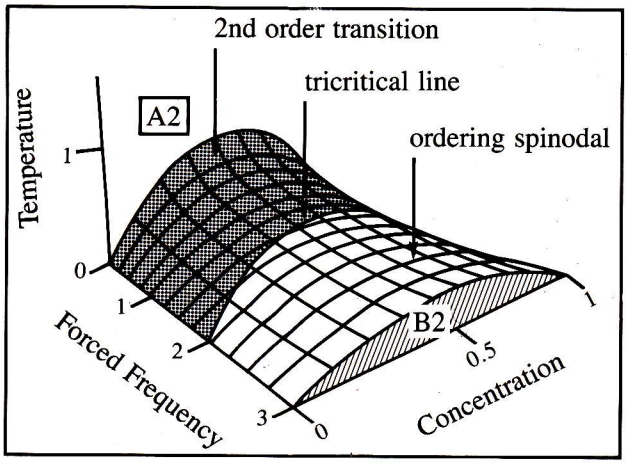

Fig. 7:
Order disorder transition surface in the Temperature, Concentration, External forcing diagram for the B2 structure. Below this surface, the compound is ordered. Beyond the tricritical line, the transition becomes first order. For the sake of clarity, only the ordering spinodal surface is shown in this area.

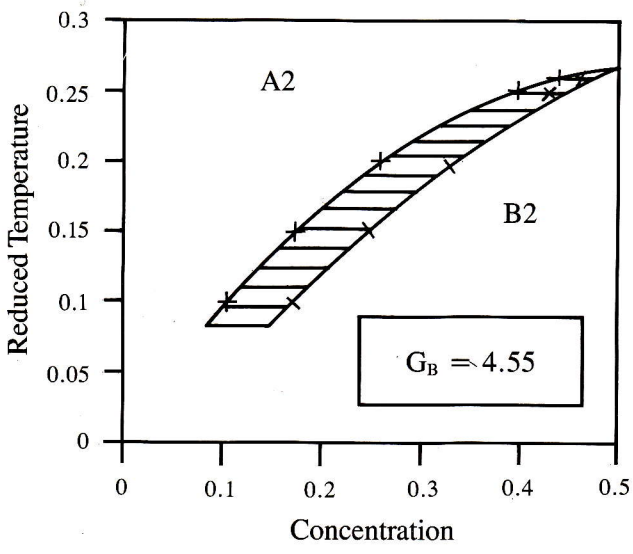

Fig. 8:
The two-phases field in the temperature-concentration plane at fixed forcing (G = 4.55).

Fig. 9:
Typical computed dynamical-equilibrium phase diagrams for compounds with a FCC lattice.

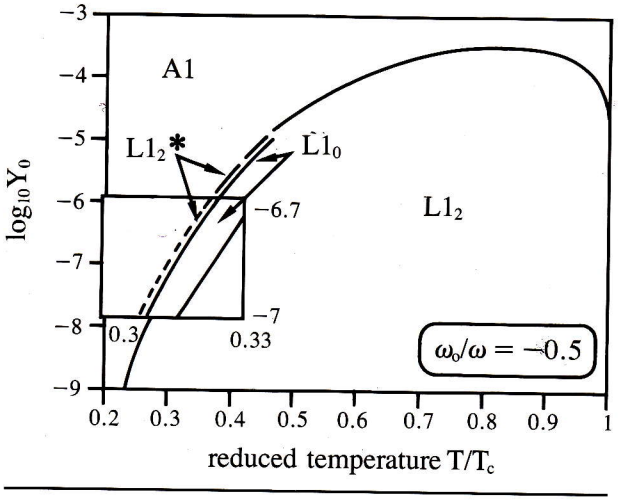

Fig. 9a:
Stability domains of various structures of stoichiometric A3B compound on the FCC lattice;

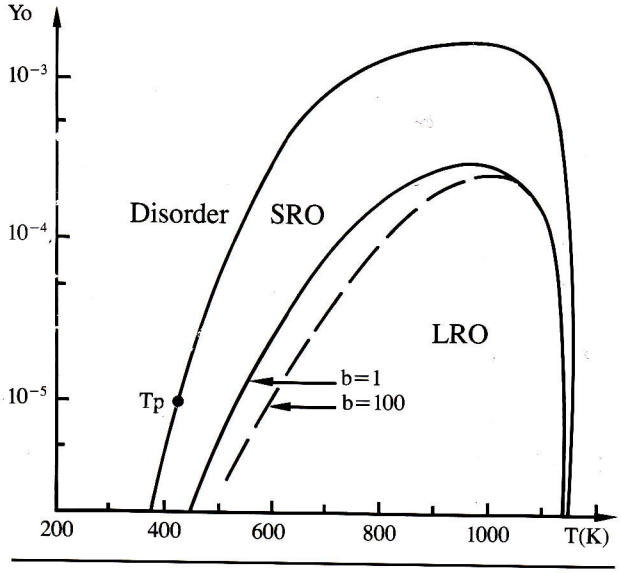

Fig. 9b:
Stability domains of "long range" ordered (LRO) and "short range" ordered (SRO) structures on the FCC lattice; notice the large effect of the cascade size b on the location of the boundary between the domains of stability of the SRO and LRO ordering.

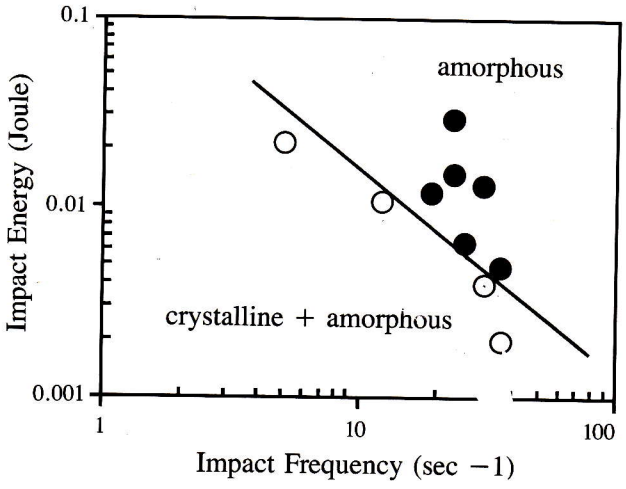

Fig. 10:
In a vibrating frame grinder, a hard ball hits the metallic powder periodically in time; in the device used by Chen et al. [5], the energy of the ball at the impact and the impact frequency can be adjusted independently. As shown on the map above, full amorphization of the $Ni_{10}Zr_7$ compound is only obtained beyond a minimum injected power density.

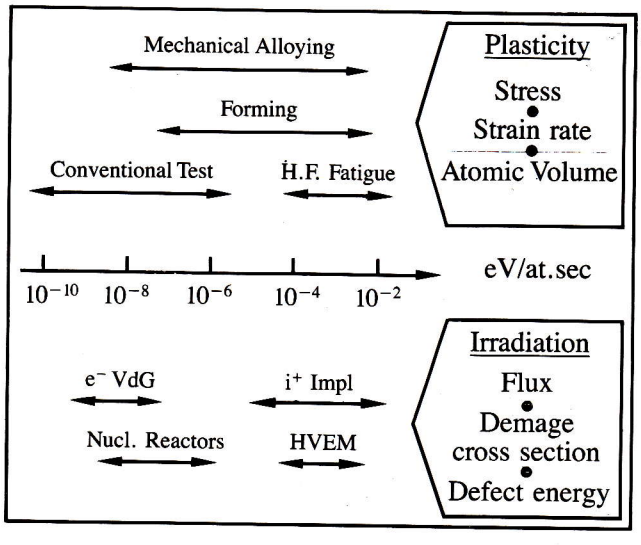

Fig. 11:
Typical power densities injected in solids under various processing or operating conditions. The unit used is the electron Volt per atom and per second.